

on microscope slides, which were then treated with ribonuclease A (0.5 mg/ml) for 10 min at 37°C. Chromosomal DNA was stained with Hoechst 33258 (0.5 µg/ml; Sigma) in 2× standard saline citrate (SSC) for 15 min at room temperature. Slides were then exposed to 365-nm ultraviolet (UV) light (Stratalinker 1800 UV irradiator) for 25 to 30 min. The BrdU/BrdC-substituted DNA was digested with Exonuclease III (3 U/µl; Promega) in 50 mM tris-HCl (pH 8.0), 5 mM MgCl₂, and 5 mM dithiothreitol for 10 min at room temperature. Chromosomes were briefly denatured in 70% formamide, 2× SSC at 70°C (1 min) and then dehydrated through a cold ethanol series (70%, 85%, and 100%). A (TTAGGG)_n probe was synthesized, labeled with Cy3 as in (22), and hybridized to the now single-stranded chromosomal target DNA, as in (5). Chromosomes were counterstained with the blue-fluorescing dye 4',6-diamidino-2-phenylindole (DAPI).

18. To be scored as a telomeric fusion, the DAPI signal had to be continuous through the point of fusion, with the

two telomeres fused into a single FISH signal. The results of hybridization analysis of HTC75 clones were confirmed in two independent laboratories. Mitotic spreads were examined with Zeiss Axiophot microscopes equipped for epifluorescence, with either a 100-watt high-pressure mercury (OSRAM) or a 75-watt mercury-xenon light source (Hamamatsu). DAPI and Cy3 excitor/dichroic/barrier filter sets (Omega Optical) were used to detect counterstained chromosomes and telomere signals, respectively. For mouse chromosomes, which tend to have large (bright) telomeres, fluorescent specimens were observed directly through the oculars of the microscope. Digital images of human chromosomes were captured with a SensSys A2S black and white charge-coupled device video camera (Photometrics), controlled by an Apple G3 computer, running Powergene MacProbe analysis software (Applied Imaging). DAPI and Cy3 channels were pseudocolored (blue and red, respectively) before being merged to produce the images shown.

19. A. H. Kurimasa et al., *Proc. Natl. Acad. Sci. U.S.A.* **96**, 1403 (1999).

20. E. H. Goodwin, J. Meyne, S. M. Bailey, *Cytogenet. Cell Genet.* **63**, 253 (1993).
21. S. M. Bailey, J. Meyne, E. H. Goodwin, in *DNA Damage and Repair*, J. Nickoloff, M. Hoekstra, Eds. (Humana Press, Totowa, NJ, 2001), vol. 3, chap. 14.
22. J. Meyne, E. H. Goodwin, *Chromosoma Res.* **3**, 375 (1995).
23. M. N. Cornforth, R. L. Eberle, *Mutagenesis* **16**, 85 (2001).
24. E. H. Goodwin, J. Meyne, S. M. Bailey, D. Quigley, *Chromosoma* **104**, 345 (1996).
25. We thank T. de Lange for the HTC75 cell lines and R. Eberle for expert technical assistance. Supported by grants from the Department of Energy/Office of Biological and Energy Research (W-7405-ENG-36, ER62684, and DEAC03-76SF00098), the National Cancer Institute (CA76260), the U.S. Army (DAMD17-97-1-7165), and NIH (AG-917709 and CA50519).

8 May 2001; accepted 3 August 2001

Dendrodendritic Inhibition Through Reversal of Dopamine Transport

Björn H. Falkenburger, Karen L. Barstow, Isabelle M. Mintz*

Synapses in the central nervous system are usually defined by presynaptic exocytotic release sites and postsynaptic differentiations. We report here a demonstration of dendrodendritic inhibition that does not engage a conventional synapse. Using amperometric and patch-clamp recordings in rat brain slices of the substantia nigra, we found that blockade of the dopamine transporter abolished the dendritic release of dopamine and the resulting self-inhibition. These findings demonstrate that dendrodendritic autoinhibition entails the carrier-mediated release of dopamine rather than conventional exocytosis. This suggests that some widely used antidepressants that inhibit the dopamine transporter may benefit patients in the early stages of Parkinson's disease.

Dopaminergic neurons of the substantia nigra are important modulators of basal ganglia function. Their degeneration leads to severe motor and cognitive deficits in Parkinson's disease (1, 2). They exert their influence distally, in the striatum, globus pallidum, and subthalamus (3), through the release of dopamine at axon terminals, and locally, in the substantia nigra, through the dendritic release of dopamine (4–6). Because dopamine hyperpolarizes dopaminergic neurons (7), it is widely accepted that the dendritic release of dopamine primarily leads to the autoinhibition of dopaminergic neurons (8), yet this has never been shown. Dopamine efflux has been documented in dendrites stimulated by high K concentrations (4, 9, 10), glutamate (11), amphet-

amine (10), and large electrical fields (12), and the molecular steps coupling dopamine autoreceptor activation to inhibition have also been identified (7). Inhibitory postsynaptic potentials (IPSPs) indicating a physiological response to released dopamine have not been seen in the substantia nigra.

We addressed this issue with patch-clamp and amperometric recording methods (13). To trigger release by a large population of dendrites, we chose to stimulate the subthalamic nucleus, because its neurons provide a robust glutamatergic input to nigral dopaminergic cells (14), and its activation in vivo increases extracellular dopamine in the substantia nigra (15, 16).

Subthalamic neurons can be stimulated in vitro to produce measurable release of dopamine in the substantia nigra (Fig. 1A). Amperometric recordings in the pars reticulata revealed that subthalamic stimulation elicited small but reproducible current transients (2.3 ± 0.7 pA, $n = 14$), indicating an increase in extracellular dopamine of about

15 to 20 nM (17). These transients showed greater amplitude in the pars reticulata, consistent with the large number of subthalamic terminals reported in this region (7).

To study the postsynaptic effects of released dopamine, we selected a subset of dopaminergic neurons whose cell bodies, located in the pars reticulata (3), may lie close to releasing dendrites (Fig. 1B, cell B in upper panel). These neurons were identified by their characteristic firing properties, morphology, or positive labeling by antibodies to tyrosine hydroxylase (13). In control conditions, they responded to repetitive subthalamic stimulation with summating monosynaptic excitatory postsynaptic potentials (EPSPs) that were followed by a slow, delayed hyperpolarization (Fig. 1B, lower panel, $n = 152/173$). This hyperpolarization reached a peak amplitude of 6.2 ± 3.0 mV (mean \pm SEM, $n = 51$). It was reduced by the D2 receptor antagonist sulpiride (on average by $73.3 \pm 15.1\%$, $n = 15$). Hence, for a small contingent of dopaminergic neurons, these findings establish a clear and reliable IPSP in response to dendritically released dopamine.

Dopaminergic neurons of the pars compacta never displayed such IPSPs in control conditions (Fig. 1C, left panel). We assumed that this apparent lack of response to dopamine might reflect the bias of our recording conditions, which favor detection of somatic synaptic potentials and actively amplified dendritic EPSPs over that of remote IPSPs that attenuate through passive propagation. Consistent with this hypothesis, in every tested cell, the inhibitory response to released dopamine was uncovered after partial blockade of the subthalamic EPSP with the glutamate receptor antagonist D(-)-2-amino-5-phosphopentanoic acid (D-AP5, 50 µM) and 6-cyano-7-nitroquinoxaline-2,3-dione (CNQX, 5 µM) (Fig. 1C, left panel, $n = 21$). These

Department of Pharmacology and Experimental Therapeutics, Boston University Medical Center, Boston, MA 02118, USA.

*To whom correspondence should be addressed. E-mail: imintz@bu.edu

REPORTS

antagonists, which reduced the subthalamic EPSPs by $88.5 \pm 5.1\%$ ($n = 21$), did not interfere with the ability of the subthalamic afferents to stimulate dendrites and trigger

dopamine release, presumably through the activation of metabotropic glutamate receptors (18). The hyperpolarization recorded in the presence of D-AP5 and CNQX repre-

sented a well-isolated dopamine-mediated inhibition, which was little affected by the γ -aminobutyric acid type B (GABA_B) receptor antagonist saclofen but was almost completely blocked by sulpiride ($93.5 \pm 5.1\%$ reduction, $n = 5$) (Fig. 1C, right panel). It resembles, in amplitude and duration, the hyperpolarization that is occasionally seen in dopaminergic neurons of the ventral tegmental area after direct electrical stimulation (19).

These data demonstrate that dopaminergic neurons of the substantia nigra respond to the dendritic release of dopamine with the expected autoinhibition. This finding applies to the small contingent of dopaminergic neurons scattered in the pars reticulata, as well as the main population of dopaminergic cells in the pars compacta, from which most of the dopaminergic innervation of the basal ganglia originates (3).

Reliable detection of autoinhibitory potentials allowed us to investigate the mechanisms by which dendrites release dopamine when they are stimulated synaptically. In dendrites exposed to high K concentrations (4), dopamine efflux is a Ca-dependent process that likely involves exocytosis. However, because dopamine-containing dendrites lack the morphological structures normally associated with exocytosis (6), other mechanisms have been considered. In particular, a Ca-independent efflux of dopamine occurs in neurons stimulated with veratridine (9) or amphetamine (10) through reversal of the dopamine transporter.

To differentiate between these two mechanisms, we used the dopamine transporter antagonist 1-[2-(diphenyl-methoxy)-ethyl]-4-(3-phenylpropyl)piperazine (GBR12935), a potent and selective inhibitor of dopamine bidirectional transport (20, 21). Because dopamine uptake contributes to the clearance of dopamine in the substantia nigra (22), blockade of the dopamine transporter is expected to decrease dopamine uptake and potentiate dopamine actions if release is exocytotic. On the contrary, if release occurs through a reversal of transport, inhibitors of dopamine transport will prevent release altogether, hindering any activation of dopaminergic IPSPs.

GBR12935, applied at low concentration (10 nM), inhibited the late IPSP triggered by subthalamic stimulation both in pars reticulata and pars compacta dopaminergic neurons (Fig. 2, $n = 7$). Figure 2A illustrates the effect of GBR12935 on the IPSP recorded in a dopaminergic neuron from the pars reticulata. In these cells, the magnitude of this effect was variable, because a significant fraction of the inhibition was often produced, after subthalamic stimulation, through GABA_B receptor activa-

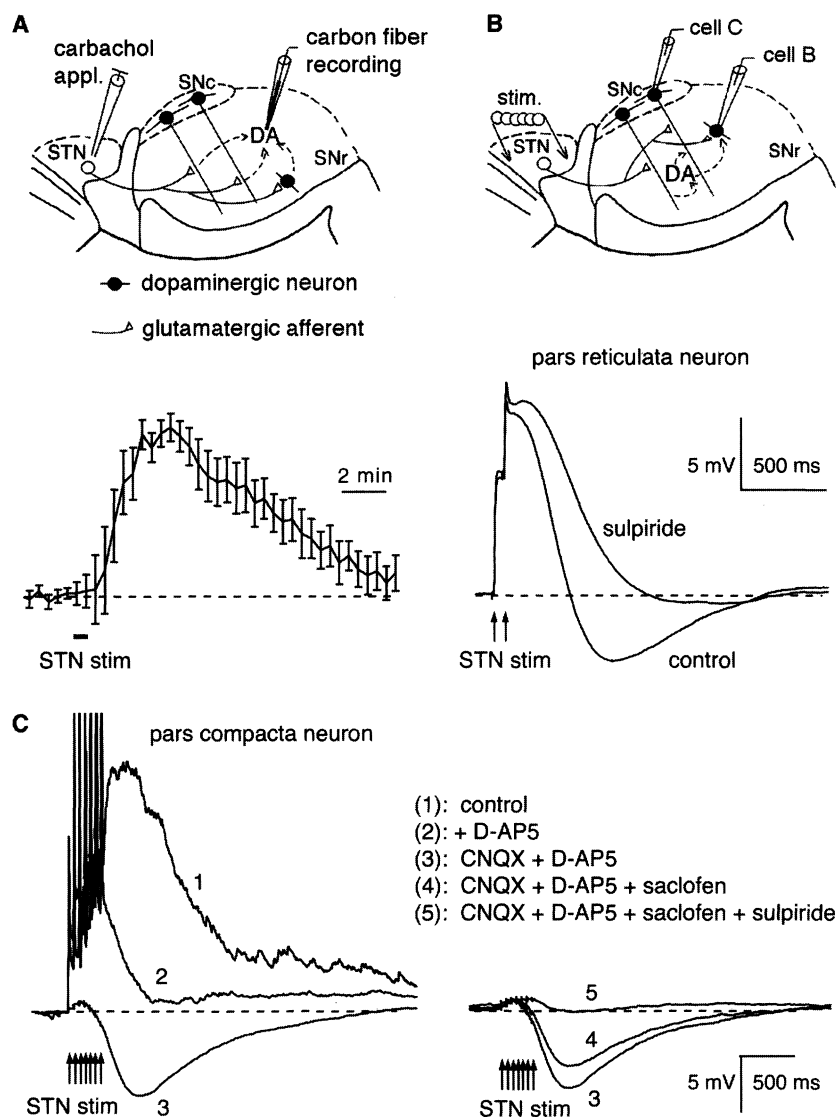


Fig. 1. (A and B) Subthalamic afferents trigger dopamine release and autoinhibition in dopaminergic neurons of the substantia nigra. (A) Amperometric detection of extracellular dopamine upon subthalamic stimulation of dopaminergic dendrites. The subthalamic nucleus was stimulated by pressure-application of a solution containing carbachol (10 mM) and NaCl (154 mM). Dopamine oxidation currents were detected with a carbon fiber (diameter 30 μ m, length 100 μ m) set at a potential of +800 mV and positioned in the substantia nigra pars reticulata. The data were recorded digitally (1-Hz filter, sampling interval 9 ms). To increase the signal-to-noise ratio by a factor of 10, we increased the initial sampling interval from 9 ms to 1 s by averaging consecutive series of 111 points. Off-line analysis and illustration were performed with the program IGOR. (B) Autoinhibition of a dopaminergic neuron recorded in the substantia nigra pars reticulata. Top: The subthalamic nucleus was stimulated by passing small currents (10 μ A to 1 mA) between two platinum wires (diameter 10 μ m) positioned \sim 200 μ m apart. Current-clamp recordings of pars reticulata (SNr) and pars compacta (SNc) neurons monitored the response of individual cells to released dopamine (2-kHz filter, sampling interval 1 ms). Bottom: Summating EPSPs and late IPSP elicited by dual stimulation of the subthalamic nucleus, before and after addition of sulpiride (1 μ M). The trace recorded in the presence of sulpiride was offset by +3 mV [baseline membrane potential (BMP) was -62 mV and -65 mV, before and after sulpiride]. (C) Autoinhibition of a dopaminergic neuron in the substantia nigra pars compacta. Trace 1: control conditions (BMP = -65 mV). Trace 2: after addition of D-AP5 (50 μ M) (BMP = -68 mV). Trace 3: in the presence of D-AP5 and CNQX (5 μ M) (BMP = -67 mV). Trace 4: after addition of saclofen (20 μ M) to the previous antagonists (BMP = -67 mV). Trace 5: after addition of sulpiride (1 μ M) to saclofen, D-AP5, and CNQX (BMP = -70 mV). The cell was injected with a constant current of -10 pA.

REPORTS

tion (23). Results in the pars compacta dopaminergic neurons were quantitatively more consistent, because we combined application of D-AP5 (50 μ M), CNQX (5 μ M), and saclofen (20 μ M) to isolate their dopamine-mediated autoinhibitory potentials. GBR12935 nearly abolished the late IPSPs (which were reduced by $94.4 \pm 5.0\%$, mean \pm SEM, $n = 3$). This action was fully reversible. The hyperpolarization, which was recovered after prolonged washout of GBR12935, amounted to $97.8 \pm 5.9\%$ of the control value ($n = 4$, including 1 pars reticulata and 3 pars compacta neurons), and it was abolished by sulpiride ($n = 4$). The experiment of Fig. 2B recapitulates these findings in a single dopaminergic neuron from the pars compacta. The left panel illustrates the unmasking of the hyperpolarization, elicited by subthalamic stimulation, after application of D-AP5 and CNQX. The right panel describes, in the same cell, the IPSP as (i) insensitive to the GABA_B antagonist saclofen, (ii) completely and reversibly blocked by GBR12935 (10 nM), and (iii) abolished after blockade of D2 receptors with sulpiride (1 μ M).

Other blockers of the dopamine transporter, (1-{2-[bis(4-fluorophenyl)methoxy]ethyl}-4(3-phenylpropyl)piperazine (GBR12909, $n = 4$) and 2- β -carboxymethoxy-3- β -(4-fluorophenyl)tropane (β -CFT, $n = 4$), also abolished the subthalamic IPSP recorded in the same conditions (Fig. 2, C and D). In contrast, this IPSP was not affected by fluoxetine, an antagonist of the serotonin transporter (Fig. 2C, $n = 3$), or by desipramine, an antagonist of the norepinephrine transporter (Fig. 2D, $n = 3$) (24).

Amperometric detection of extracellular dopamine provided a separate demonstration that the dopamine transporter mediates dopamine release evoked by subthalamic inputs (Fig. 3A). The oxidation currents elicited (as in Fig. 1A) by subthalamic stimulation were inhibited reversibly by GBR12935 ($n = 3/3$). After application of 20 nM GBR12935 for 90 min, they were reduced by $76 \pm 6.8\%$ and they fully recovered within 2 hours after washout of GBR12935. In contrast, GBR12935 (20 nM) enhanced currents elicited by exogenously applied dopamine (by $42 \pm 20\%$ after 30 min, $n = 4$, Fig. 3B), due to inhibition of uptake. A similar enhancement was seen in Fig. 3A (bottom), which suggests that the effects of GBR12935 on release and uptake can be dissociated (25).

In addition to their distinct response to dopamine transporter antagonists, the exocytotic and carrier-mediated release of dopamine can be distinguished by distinct calcium requirements. Unlike exocytosis, dopamine transport is unaffected by remov-

al of external Ca²⁺ ions (9, 20). To emulate the subthalamic stimulation of dendrites in calcium-free conditions, we used local pressure application of glutamate (1 mM).

In the pars reticulata, glutamate applications resulted in robust and reproducible amperometric currents (10.6 ± 1.8 pA, $n = 12$) (Fig. 4). These transient currents, mea-

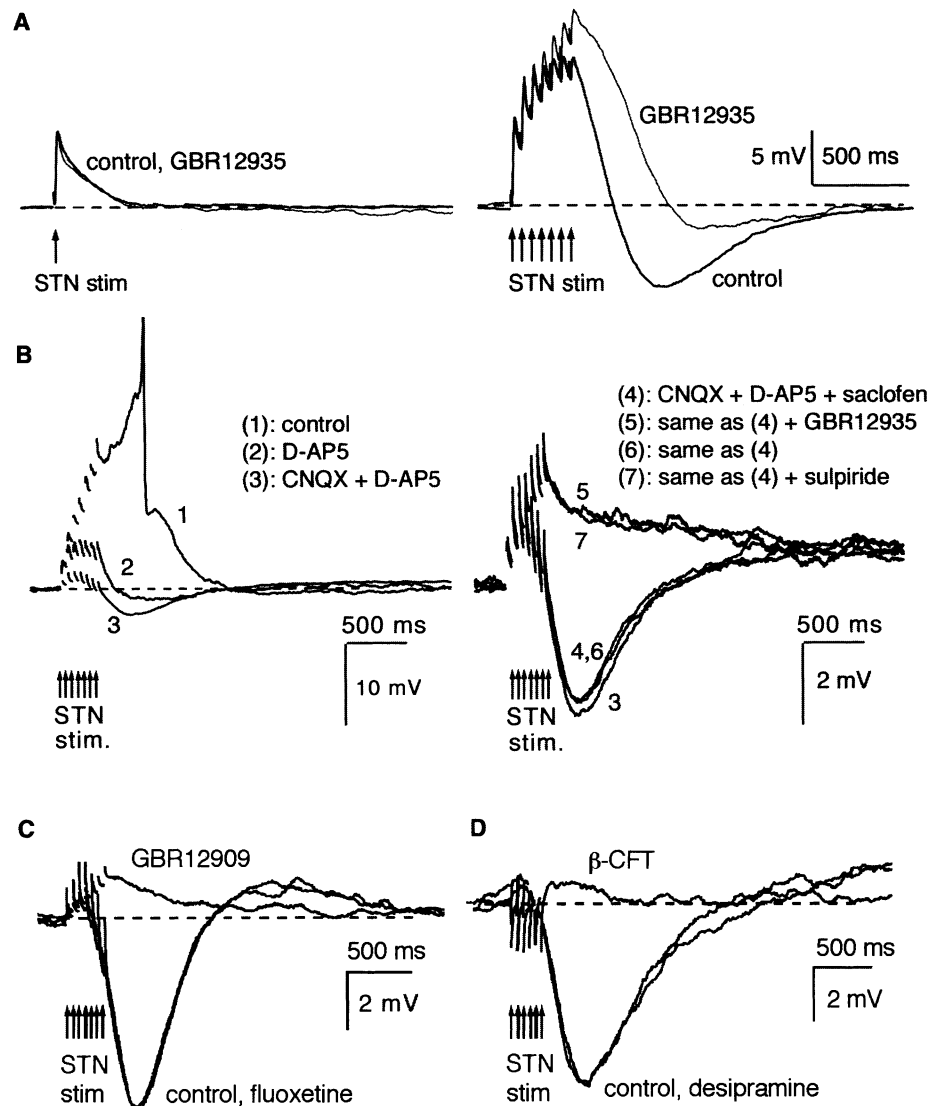


Fig. 2. Dopamine transporter antagonists block autoinhibition in dopaminergic neurons of the substantia nigra. (A) GBR12935 (10 nM) inhibition of the late IPSP elicited by subthalamic stimulation of a pars reticulata neuron. (B) GBR12935 inhibition of the late IPSP in a dopaminergic neuron of the pars compacta. Trace 1 illustrates the EPSPs triggered by subthalamic stimulation (BMP = -65 mV). To uncover the IPSP, the cell was sequentially exposed to D-AP5 (50 μ M) (trace 2, BMP = -68 mV), D-AP5 + CNQX (5 μ M) (trace 3, BMP = -67 mV), D-AP5 + CNQX + saclofen (20 μ M) (trace 4, BMP = -67 mV). The late IPSP recorded in these conditions was blocked by GBR12935 (10 nM) (trace 5, in D-AP5 + CNQX + saclofen + GBR12935, BMP = -70 mV). Blockade by GBR12935 was reversed (trace 6, in D-AP5 + CNQX + saclofen, BMP = -68 mV) and the recovered IPSP was abolished by sulpiride (1 μ M) (trace 7, in D-AP5 + CNQX + saclofen + sulpiride, BMP = -69 mV). Both cells in (A) and (B) were injected with a constant current of -10 pA. (C) GBR12909 (10 nM) inhibition of the IPSP elicited by subthalamic stimulation in a dopaminergic neuron of the pars compacta. APV (50 μ M), CNQX (5 μ M), and saclofen (20 μ M) were present throughout the experiment. Fluoxetine (100 nM) was added 20 min before GBR12909 to verify that the late IPSP was unaffected by inhibition of the serotonin transporter (BMP = -66 mV in control, in the presence of fluoxetine, and after addition of GBR12909). The cell was steadily injected with a constant current of -50 pA. (D) β -CFT (10 nM) inhibition of the late IPSP evoked by subthalamic stimulation in another dopaminergic neuron of the pars compacta. APV (50 μ M), CNQX (5 μ M), and saclofen (20 μ M) were present throughout the experiment. Desipramine (100 nM) was added 20 min before β -CFT to verify that the late IPSP was unaffected by inhibition of the norepinephrine transporter (BMP = -65 mV in control, BMP = -63 mV in the presence of desipramine, BMP = -68 mV after addition of β -CFT). The cell was steadily injected with a constant current of -20 pA.

REPORTS

sured at a carbon fiber that was positioned in the pars reticulata, signaled transient increases in dopamine levels with little contamination by other amines (17). Whereas the transient responses in the presence of 2 mM extracellular Ca decreased with each application of glutamate, the amperometric signals in calcium-free conditions were remarkably stable (26), demonstrating that glutamate receptor activation reliably triggers the calcium-independent efflux of dopamine.

Consistent with the hypothesis that glutamate stimulation of dopaminergic dendrites leads to a reversal of dopamine transport, the amperometric currents recorded in these conditions were significantly reduced (by $70 \pm 1.3\%$, $n = 4$) by GBR12935 (20 nM). The amperometric signals fully recovered, within 2 hours, after washout of the antagonist ($n = 3$), ruling out inhibition of the responses to glutamate through reduction in the carbon fiber sensitivity, depletion of the releasable pool of dopamine, or degradation of the brain slice condition. In the experiment of Fig. 4, selected for the stability of the carbon fiber electrode over the 4-hour length of the recordings, GBR12935 nearly abolished the transients evoked by glutamate applications. Interestingly, it produced dissociated effects on the basal levels of dopamine and the transient increases triggered by glutamate application (25). As predicted if low concentrations of GBR12935 preferentially affect dopamine uptake, GBR12935 initially increased the baseline levels of dopamine and enhanced the amperometric signal evoked by glutamate application. However, the subsequent responses to glutamate were reduced. After 90 min of GBR12935 application, their inhibition amounted to $\sim 90\%$ of the control current. Recovery from block was slow but complete and was accompanied by a parallel return of the dopamine baseline level to its initial value. These data demonstrate that, upon glutamate receptor activation, dopaminergic dendrites release dopamine in calcium-free conditions through reversal of dopamine transport.

These data show that under physiological conditions, reversal of dopamine transport occurs when dopamine-containing dendrites are stimulated by their subthalamic afferents. Although they explain the lack of dendrodendritic synapses reported in the pars reticulata (6), our findings were largely unexpected. First, recent amperometric studies (27) clearly establish the occurrence of dopamine exocytosis in the substantia nigra. Second, inside-out transport of dopamine had only been documented in nonphysiological conditions that seemed unlikely to be matched in dendrites stimulated synaptically (9, 20).

The direction and magnitude of dopamine transport depends on membrane potential and

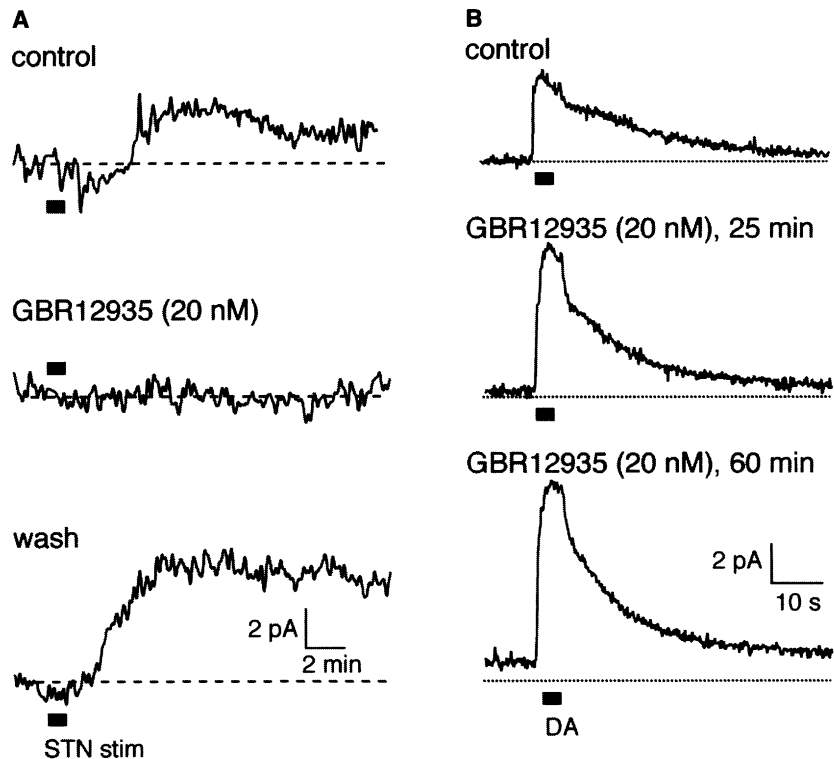


Fig. 3. GBR12935 inhibits the dendritic release of dopamine evoked by subthalamic stimulation and enhances the response to exogenously applied dopamine. (A) Amperometric currents were evoked in the pars reticulata after carbachol stimulation of the subthalamic nucleus (as in Fig. 1A), in control condition (top), after the application of 20 nM GBR12935 (middle) and 15 min after washout of the antagonist (bottom). Calibration of the carbon-fiber electrode was 9 nM dopamine/pA. (B) Amperometric currents evoked by pressure application of dopamine (1 μ M, in 154 mM NaCl, with 1 mM D-cysteine to prevent dopamine oxidation), in control (top), 25 min (middle), and 60 min (bottom) application of 20 nM GBR12935. Calibration of the carbon-fiber electrode was 16 nM dopamine/pA.

the Na^+ and Cl^- ion gradients (28). Our results imply that subthalamic EPSPs depolarize dendrites beyond the reversal potential for dopamine transport. Considering the geometry of the dendrites (their large surface-to-volume ratio), it is likely that increases in intracellular Na and membrane depolarization both contribute to reversal of dopamine transport. One can easily imagine that Na influx through glutamate-gated channels and voltage-gated Na channels (29) raises the intracellular Na concentration significantly, bringing the reversal potential for dopamine transport closer to the cell resting membrane potential.

The carrier-mediated release of dopamine bypasses the classic requirements for transmission at conventional synapses. Considering the wide distribution of the dopamine transporter (30), every dendritic compartment is a potential release site for dopamine. Rather than being defined structurally by their exocytotic machinery, the dendritic release sites for dopamine may therefore be allocated dynamically, in space and time, by propagating Na action potentials (29) and other dendritic regenerating responses (31). Locally, it is unclear whether the activity of the dopamine transporter itself

shortens dopamine efflux; released dopamine would be expected to hyperpolarize releasing dendrites, thereby promoting its own uptake (32). Because the release of dopamine through the transporter is intrinsically transient, it is well suited for shaping the phasic responses of dopaminergic neurons in the substantia nigra during reward and attention-shifting tasks (33), as well as their bursting behavior (7).

Dopamine transporter inhibitors are widely used in the treatment of depression, attention-deficit hyperactivity disorder, and addiction (34). Disruption of carrier-mediated release of dopamine (in midbrain nuclei) could be another mechanism by which dopamine transporter antagonists exert their therapeutic effects, in addition to their known facilitation of dopaminergic transmission at axon terminals. Such a mechanism of action predicts a novel clinical application for dopamine transporter inhibitors as neuroprotective agents in the early stages of Parkinson's disease. Because subthalamic afferents trigger the carrier-mediated release of dopamine in the substantia nigra, their hyperactivity in Parkinson's patients (2) likely results in excessive release of dopamine. Considering dopamine neurotoxicity (35), inhibition of such release by dopamine trans-

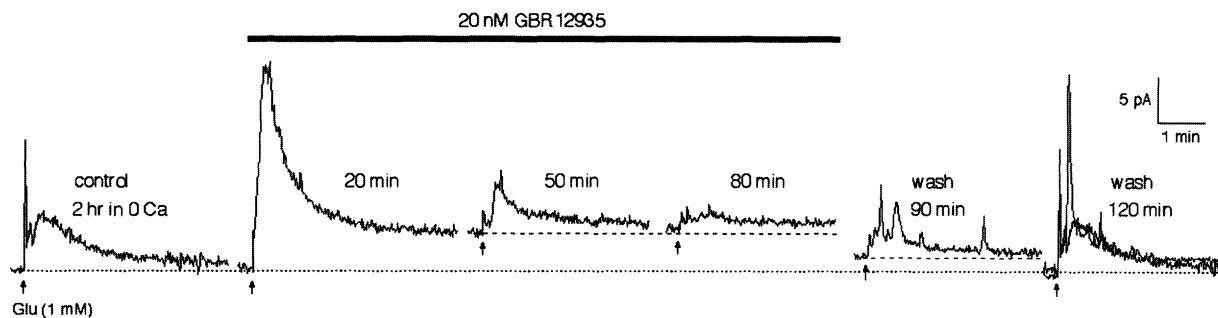


Fig. 4. GBR12935 inhibits the Ca-independent release of dopamine triggered by glutamate application. Traces represent individual amperometric responses to glutamate (1 mM) application in control calcium-free condition, in the presence of GBR12935 (20 nM), and after washout of the blocker. The final trace is superimposed with the control response to illustrate the full recovery of the evoked signal and the baseline to their initial values. Amperometric signals were detected and recorded as

in Fig. 1A, but dendrites were stimulated directly by pressure-application of glutamate through a glass pipette that was positioned in the substantia nigra pars reticulata and filled with glutamate (1 mM) and NaCl (154 mM). Each pulse (9 s, 30 psi, every 30 min) applied ~60 nl of the glutamate-containing solution. The whole experiment was carried out in calcium-free solution (26). Calibration of the carbon fiber electrode was 140 nM dopamine/pA.

porter blockers may slow the degeneration of dopaminergic neurons in Parkinson's disease.

References and Notes

1. M. Graybiel, T. Aosaki, A. W. Flaherty, M. Kimura, *Science* **265**, 1826 (1994).
2. A. M. Lozano, A. E. Lang, W. D. Hutchison, J. O. Dostrovsky, *Curr. Opin. Neurobiol.* **8**, 783 (1998).
3. A. Björklund, O. Lindvall, *Handbook of Neuroanatomy* (Elsevier Science, Amsterdam, 1984), vol. 2, part 1, pp. 55–122.
4. L. B. Geffen, T. M. Jessel, A. C. Cuello, L. L. Iversen, *Nature* **260**, 258 (1976).
5. A. Cheramy, V. Leviel, J. Glowinski, *Nature* **16**, 415 (1981).
6. M. Wassef, A. Berod, C. Sotelo, *Neuroscience* **6**, 2125 (1981).
7. M. L. Pucak, A. A. Grace, *Crit. Rev. Neurobiol.* **9**, 67 (1994).
8. P. M. Groves, C. J. Wilson, S. J. Young, G. V. Rebec, *Science* **190**, 522 (1975).
9. A. Elverfors, J. Jonason, G. Jonason, H. Nissbrandt, *Synapse* **26**, 359 (1997).
10. A. F. Hoffman, G. A. Gerhardt, *J. Pharmacol. Exp. Ther.* **289**, 455 (1999).
11. R. Araneda, G. Bustos, *J. Neurochem.* **52**, 962 (1989).
12. M. E. Rice, S. J. Cragg, S. A. Greenfield, *J. Neurophysiol.* **77**, 853 (1997).
13. Amperometric and patch-clamp recording experiments were performed at room temperature, using 400- μ m-thick parasagittal brain slices from 10- to 16-day-old rats. For patch-clamp recording experiments, the subthalamic nucleus was stimulated electrically. Because amperometric detection of dopamine is constrained by the carbon fiber sensitivity, we were unable to detect the small, localized changes in dopamine concentration that were triggered by bipolar stimulation of the subthalamus. We found that local pressure application (36 s, 20 psi) of carbachol (10 mM) to be the most effective to stimulate a large population of subthalamic neurons in synchrony (16). Each pressure application pulse resulted in the ejection of 10 nmol of carbachol. As a result, the amperometric signals were much slower than the dopamine-mediated IPSPs. In all experiments, the control external solution contained 125 mM NaCl, 2.5 mM KCl, 2 mM CaCl₂, 1 mM MgCl₂, 26 mM NaHCO₂, 1.25 mM Na₂PO₄, 25 mM glucose, and 0.02 mM bicuculline methiodide, bubbled with a mixture of 95% O₂ and 5% CO₂ (pH = 7.4). Whole-cell current-clamp recordings of dopaminergic neurons were performed with patch pipettes filled with 108 mM K methanesulfonate, 4 mM MgCl₂, 9 mM EGTA, 9 mM Hepes (acid), 4 mM Mg-ATP, 0.3 mM GTP (tris salt), and 14 mM creatine phosphate (tris salt) (pH set to 7.4 with KOH). In these experiments, dopaminergic neurons were identified visually, by the characteristic shape of their soma and by their firing properties (36). This criterion was validated by dou-

- ble labeling (n = 6), with lucifer yellow and a monoclonal mouse antibody to tyrosine hydroxylase (37). All antagonists were bath-applied.
14. Y. Iribe, K. Moore, K. C. Pang, J. M. Tepper, *J. Neurophysiol.* **82**, 925 (1999).
15. I. Mintz, C. Hammond, B. Guibert, V. Leviel, *Brain Res.* **376**, 406 (1986).
16. G. Rosales, G. Flores, S. Hernández, D. Martínez-Fong, J. Aceves, *Brain Res.* **645**, 335 (1994).
17. The oxidation currents produced by released dopamine upon subthalamic stimulation were too small to be detected with fast-scan voltametry or high-speed chronoamperometry, techniques that are otherwise preferred as they provide more specific monitoring of extracellular dopamine levels. In our experimental settings, however, we can infer selectivity indirectly. Other amines like 3,4-dihydroxyphenylacetic acid (DOPAC) (38), serotonin (39), and norepinephrine (40) are present in the substantia nigra and will be oxidized in our experimental settings. However, while they may contribute to baseline oxidation currents, they are not likely to affect the transient amperometric signals evoked by dendritic stimulation. In the case of serotonin and norepinephrine, axon terminals that release these monoamines in the substantia nigra are unlikely to synchronize exocytosis upon stimulation of the subthalamic afferents (Figs. 1 and 3) or in calcium-free conditions (Fig. 4). In the case of DOPAC, its production by dopamine metabolism is too slow to affect the transient signals evoked by dendritic stimulation (38). In all instances, the sensitivity of the amperometric signals to GBR12935 provided additional control for selectivity. To ensure selective inhibition of the dopamine transporter with no effects on the transporters for serotonin and norepinephrine, we used low concentrations of GBR12935 (10 to 20 nM), similar to its IC₅₀ for inhibition of dopamine release (20) and uptake (21) through the dopamine transporter (27).
18. After blockade of N-methyl-D-aspartate (NMDA)-gated and non-NMDA-gated channels, the subthalamic EPSP of SNc and SNr dopaminergic neurons was abolished by 7-(hydroxymino)cyclopropa[b]chromen-1a-carboxylate ethyl ester (PCPCOEt, 100 μ M), an antagonist of type 1 metabotropic glutamate receptors (n = 4). The late IPSP decreased in parallel, suggesting that mGluR1 receptor activation triggered dopamine release in these conditions.
19. S. W. Johnson, R. A. North, *J. Physiol. (London)* **450**, 455 (1992).
20. A. J. Eshleman, R. A. Henningsen, K. A. Neve, A. Janowsky, *Mol. Pharmacol.* **45**, 312 (1994).
21. R. B. Rothman et al., *Synapse* **14**, 34 (1993).
22. F. Hoffman, C. R. Lupica, G. A. Gerhardt, *J. Pharmacol. Exp. Ther.* **287**, 487 (1998).
23. In control conditions, SNr dopaminergic neurons displayed complex subthalamic IPSPs comprising a GABA_B receptor-mediated component (sensitive to saclofen)

- and a dopamine-mediated autoinhibitory potential (blocked by sulpiride) (Fig. 1). Addition of APV (50 μ M) and CNQX (5 μ M) reduced the size of the saclofen-sensitive IPSP by 60 to 100%, suggesting that these IPSPs involved, to some degree, local interneurons that were activated by subthalamic inputs.
24. The concentration and length of application of fluoxetine (Fig. 2C) and desipramine (Fig. 2D) were determined in a set of preliminary experiments that tested their effect on the carrier-mediated release of serotonin in the raphe nucleus and the carrier-mediated release of norepinephrine in the locus coeruleus. Fluoxetine (100 nM for 20 min) abolished the amperometric signal evoked in the raphe nucleus by pressure application of glutamate (1 mM). Similarly, desipramine (100 nM, 30 min) significantly reduced the amperometric signals evoked in the locus coeruleus by glutamate (1 mM). These experiments were performed in the absence of external calcium.
25. In experiments using carbon fibers positioned deep in the slice (Figs. 3A and 4), the time course of GBR12935 effect was determined by diffusion. The slow changes in GBR12935 concentration allowed to resolve its dissociated effect on dopamine uptake (enhancement of the signals seen upon washout in Fig. 3A or upon GBR12935 application in Fig. 4) before the blockade of dopamine release (steady-state inhibition of the signals evoked by subthalamic stimulation in Fig. 3A and glutamate application in Fig. 4). Because GBR12935 binds to a single site with high affinity (dissociation constant ~ 3 nM) (41), it may inhibit substrate binding to extracellular sites and prevent uptake at low concentrations, and it may effectively lock in the carrier and prevent its inside-out translocation at high concentrations.
26. In the presence of 2 mM extracellular calcium, glutamate application triggered a significant increase in extracellular dopamine concentration. Subsequent applications were less effective, suggesting depletion of the calcium-dependent releasable pool of dopamine. However, upon complete removal of external calcium, glutamate applications triggered small but reliable increases in dopamine levels that were routinely maintained for hours. For these experiments, we chose a low concentration of glutamate (1 mM) to mimic the glutamate profile in the synaptic cleft (42). The calcium-free external solution contained 125 mM NaCl, 2.5 mM KCl, 3 mM MgCl₂, 26 mM NaHCO₂, 1.25 mM Na₂PO₄, 25 mM glucose, 0.02 mM bicuculline methiodide, and 1 mM EGTA, bubbled with a mixture of 95% O₂ and 5% CO₂ (pH = 7.4) (experiments of Figs. 3B and 4).
27. E. H. Jaffe, A. Marty, A. Schulte, R. H. Chow, *J. Neurosci.* **18**, 3548 (1998).
28. M. S. Sonders, S. G. Amara, *Curr. Opin. Neurobiol.* **6**, 294 (1996).
29. M. Häusser, G. Stuart, C. Racca, B. Sakmann, *Neuron* **15**, 637 (1995).

30. M. J. Nirenberg, R. A. Vaughan, G. R. Uhl, M. J. Kuhar, V. M. Pickel, *J. Neurosci.* **16**, 436 (1996).
 31. R. Llinas, S. A. Greenfield, H. Jahnsen, *Brain Res.* **294**, 127 (1984).
 32. In preliminary experiments (in calcium-free conditions), applications of sulpiride did not affect the time course of the amperometric signals elicited by local application of glutamate. This finding may reflect technical limitations (the carbon fiber may sample the asynchronous release of dopamine over a large area, providing a poor time resolution of the release process) or the fact that diffusion rather than dopamine uptake shapes the amperometric response to glutamate application, in our experimental conditions (in Fig. 3B, GBR12935 had little effect on the decaying phase of dopamine profile after exogenous application of dopamine). A definite answer awaits more local measurements of dopamine release by single dendrites.
 33. W. Schultz, *J. Neurophysiol.* **80**, 1 (1998).
 34. B. Giros, M. G. Caron, *Trends Pharmacol. Sci.* **14**, 43 (1992).
 35. C. T. Lai, P. H. Yu, *Biochem. Pharmacol.* **53**, 363 (1997).
 36. W. H. Yung, M. A. Häusser, J. J. B. Jack, *J. Physiol. (London)* **436**, 643 (1991).
 37. K. L. Barstow, thesis, Boston University School of Medicine (2001).
 38. M. Buda et al., *Eur. J. Pharmacol.* **73**, 61 (1981).
 39. A. Dray, T. J. Gonye, N. R. Oakley, T. Tanner, *Brain Res.* **113**, 45 (1976).

40. G. L. Collingridge, T. A. James, N. K. MacLeod, *J. Physiol. (London)* **290**, 44P (1979).
 41. N. A. Sharif et al., *Neurochem. Int.* **21**, 69 (1992).
 42. J. D. Clements, R. A. Lester, G. Tong, C. E. Jahr, G. L. Westbrook, *Science* **258**, 1498 (1992).
 43. We thank B. P. Bean for his generous loan of equipment and comments on the manuscript, S. E. Leeman and G. G. Blasdel for many helpful editorial suggestions, and U. C. Dräger and R. G. Feldman for invaluable help at the beginning of this project. Supported by a fellowship from the John Nicholl fund (K.L.B.), a "Studienstiftung des deutschen Volkes" scholarship (B.H.F.), and grants from the APDA and NIH (R01-3445) (I.M.M.).

4 June 2001; accepted 2 August 2001

A Cortical Area Selective for Visual Processing of the Human Body

Paul E. Downing,^{1*} Yuhong Jiang,² Miles Shuman,² Nancy Kanwisher^{2,3}

Despite extensive evidence for regions of human visual cortex that respond selectively to faces, few studies have considered the cortical representation of the appearance of the rest of the human body. We present a series of functional magnetic resonance imaging (fMRI) studies revealing substantial evidence for a distinct cortical region in humans that responds selectively to images of the human body, as compared with a wide range of control stimuli. This region was found in the lateral occipitotemporal cortex in all subjects tested and apparently reflects a specialized neural system for the visual perception of the human body.

One of the most fundamental questions about visual object recognition in humans is whether all kinds of objects are processed by the same neural mechanisms, or whether instead some object classes are handled by distinct processing "modules." The strongest evidence to date for a modular recognition system comes from the case of faces [(1), but see (2)]. In contrast, relatively few studies have considered the mechanisms involved in perceiving the rest of the human body. Neuropsychological reports suggest that semantic knowledge of human body parts may be distinct from knowledge of other object categories (3). In addition, functional neuroimaging studies have implicated regions of the superior temporal sulcus (STS) in the perception of biological motion (4–6) and have associated regions of left parietal and prefrontal cortices with knowledge about body parts (7). Finally, single-unit recording studies in monkeys have identified neurons in the STS

that respond selectively to the appearance of the body, including the face (8–9). None of these findings, however, provides conclusive evidence for a region in human visual cortex selectively involved in processing the appearance of human bodies. Here, we report a

series of fMRI studies that provide the first evidence for such a region.

Subjects in these experiments were scanned while viewing images of objects from several different categories. In 19 out of 19 subjects scanned, we found a region in the right lateral occipitotemporal cortex (Fig. 1) that produced a significantly stronger response when subjects viewed still photographs of human bodies and body parts than when they viewed various inanimate objects and object parts (10). We have provisionally named this candidate body-selective region the "extrastriate body area" or EBA (11). After identifying the EBA in each subject with these "localizer" scans, we then ran a new set of experimental scans in the same session, in order to measure the response of the EBA to a large number of other stimulus categories (Figs. 2 and 3). This procedure enabled us to characterize the response profile of this region to a variety of different kinds of visual stimuli (12) in order to test a number of alternatives to our hypothesis that the EBA is selectively involved in visual processing of the human body.

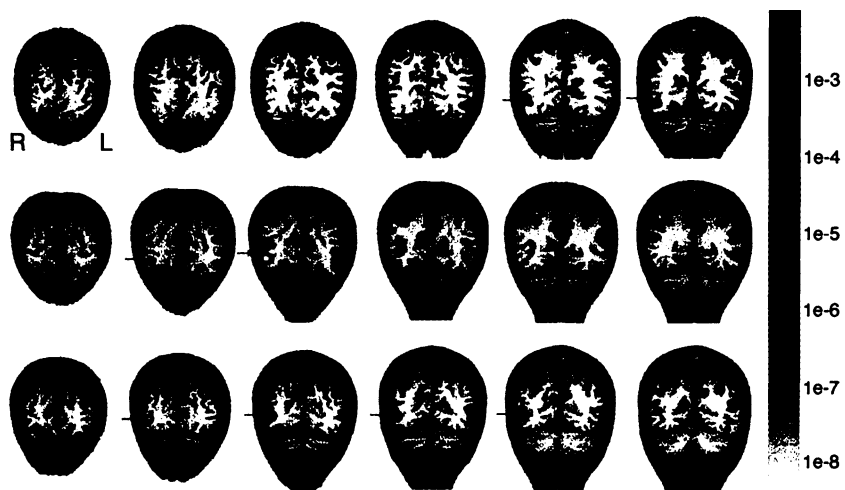


Fig. 1. EBA activations in three individual subjects. Each row shows coronal anatomical slices from a single subject, arranged from posterior (left) to anterior (right), overlaid with a statistical map showing voxels that were significantly more active for human bodies and body parts than for objects and object parts. The EBA is visible in the right occipitotemporal cortex of each subject (arrows); in some subjects an activation was also observed in the corresponding location of the left hemisphere. Scale indicates *P* value of activations in colored regions.

¹School of Psychology, Centre for Cognitive Neuroscience, University of Wales, Bangor LL57 2AS, UK.

²Department of Brain and Cognitive Sciences, Massachusetts Institute of Technology, Cambridge, MA 02139, USA. ³Massachusetts General Hospital–Nuclear Magnetic Resonance Imaging Center, 149 13th Street, Charlestown, MA 02129, USA.

*To whom correspondence should be addressed. E-mail: p.downing@bangor.ac.uk